Influence of calcium aluminate cement (CAC) on alkaline activation of red clay brick waste (RCBW)

L. Reig [a], L. Soriano [b], M.V. Borrachero [b], J. Monzó [b], J.Payá [b]

[a] EMC, Universitat Jaume I, Av. Sos Baynat s/n 12071 Castelló de la Plana, Spain.

[b] Instituto de Ciencia y Tecnología del Hormigón (ICITECH), Universitat Politècnica de València, Camino de Vera s/n 46022 Valencia, Spain.

Corresponding author: L. Reig; lreig@uji.es

Tel.: +34 964 729163

Fax: +34 964 728106

E-mail addresses: lreig@uji.es; lousomar@gmail.com; vborrachero@cst.upv.es; jmmonzo@cst.upv.es; jjpaya@cst.upv.es

Abstract

In this paper, the effect of calcium aluminate cement (CAC) additions on the alkali activation of red clay brick waste (RCBW) was studied at room temperature and at 65 ºC. RCBW was partially replaced with CAC (0 to 50 wt.%) and blends were activated with NaOH and sodium silicate solutions. The compressive strength evolution was tested on mortars and the nature of the reaction products was analysed by infrared spectroscopy, X-ray diffraction, thermogravimetric analysis, microscopic studies and pH measurements. The results show that the use of CAC accelerates the activation process of RCBW so that 50 MPa were obtained in the blended mortars containing 40 wt.% CAC cured for 3 days at room temperature. CAC did not undergo normal hydration and only the C_3AH_6 phase was identified in the pastes blended with more than 30 wt.% CAC and cured at 65ºC, while the main reaction product was a cementitious gel containing Ca and Al from CAC.

Keywords:

Ceramic waste

Waste management

Alkali-Activation

Calcium aluminate cement

Compressive strength

Microstructure

1. Introduction

Portland cement is the dominant binder used in concrete. However, the large amounts of energy and greenhouse gases emitted to the atmosphere during its production process have prompted the scientific community to propose different alternatives to reduce its environmental impact. As reviewed by Juenger et al. [1], alkali-activated binders are receiving more attention from among the different alternatives proposed, which is attributed to their excellent strength, durability and low environmental impact. Furthermore in this methodology, the solid material to be activated may be entirely (or almost entirely) composed of waste materials [1]. As described by Shi et al. [2], during the alkali-activation process, a solid silico-aluminous material is mixed with a highly concentrated alkali solution. The resulting paste is an aluminosilicate hydrate that has a three-dimensional structure, with both Al and Si tetrahedrally coordinated, and the alkali (Na or K) located in the voids of this framework, which compensate for electric charges.

A wide variety of industrial by-products and waste materials have been successfully activated by the scientific community [2-5], some of which are ceramics. Among them, Puertas et al. [6] achieved 13 MPa (compression) by the alkali activation of different types of ceramic tiles, cured at 85ºC for 24h and at 20ºC for 7 days. Payá et al. [7] also developed mortars with compressive strength values above 10 MPa by the activation of hydrated-carbonated cement cured at 65ºC. Porcelain stoneware tiles were activated by Reig et al. [8], where the addition of $Ca(OH)_2$ proved essential to obtain mortar samples with up to 36 MPa under compression (7 days at 65°C). Red clay brick waste has also been activated in a previous research work [9], where up to 50 MPa were reported under compression in mortars cured at 65ºC for 7 days. Although the development of binders by the alkali activation of ceramic materials has been extensively proved, what most of these studies have in common is that curing at high temperature was required for the activation process to take place.

In the works by Fernandez-Jimenez et al. [10] and Arbi et al. [11], calcium aluminate cement (CAC) was added to the system as a source of calcium and reactive alumina. Thus compressive strength values close to 13 MPa were obtained in the alkali-activated metakaolin pastes containing 20% CAC (cured at 85ºC for 20 h) [10]. Even higher compressive strength values (23.7 MPa) were achieved in [11] by the activation of blast furnace slag and CAC blends (80 to 20 wt.%) cured at room temperature for 2 days. Thus although CAC production consumes natural resources (bauxite and limestone), emits CO_2 to the atmosphere and requires energy to reach clinkering temperatures, moderate amounts of this cement may improve the behaviour and properties of the blended system. As Pacewska et al. [12] described, CAC is a hydraulic binder with special properties, such as rapid strength gain, good durability in high sulphate environments, resistance to fire, chemical attack and abrasion. Monocalcium aluminate (CA) is the principal active phase in CAC cement, which reacts with water to give calcium aluminate hydrates. As described by Juenger et al. [1], hydration temperature is one of the most significant parameters to influence the phases that are formed and the transition rate from metaestable to stable hydrates (conversion process). Whereas CA hydrates at environmental temperatures (15 to 25ºC) to give hexagonal phases $CaAl_2O_4 \cdot 10H_2O$ (CAH_{10}) and $Ca_2Al_2O_5 \cdot 8H_2O$ (C_2AH_8), with an increased quantity of C_2AH_8 with rising temperature, curing within the 25-40ºC range yields C_2AH_8 as the main hydration product, together with alumina gel, which crystallizes with time to gibbsite $Al(OH)_3$ (AH_3). When temperature rises above 40ºC, and especially up to 60ºC, phase $Ca_3Al_2(OH)_{12}$ (C_3AH_6) is formed (cubic phase), together with hydrous alumina, which gradually changes to gibbsite. As extensively proved by the scientific community [1,13,14], CAH_{10} and C_2AH_8 are metastable products that inevitably convert into stable C_3AH_6 and AH_3 phases depending on time, temperature, humidity or pH. The conversion of these metastable hydrates into the stable cubic phase occurs in accordance with Equations (1) and (2) [13], and is accompanied by AH_3 gel formation and the release of water (H). As a result, the porosity of the paste increases, and the strength of the material subsequently diminishes [1,13-15].

$$3CAH_{10} \rightarrow C_3AH_6 + 2AH_3 + 18H \quad (1)$$

$$3C_2AH_8 \rightarrow 2C_3AH_6 + AH_3 + 9H \quad (2)$$

Carbonation of CAC hydrates may also occur if CO_2 from the atmosphere is absorbed, which results in the formation of $CaCO_3$ and AH_3. As explained in [14], the hexagonal phases carbonate faster than the cubic one as they are less stable and dissolve CO_2 more easily. The alkaline hydrolysis, a durability problem associated with CAC, has been described in [14] also as a carbonation process which occurs with high pH values and in the presence of alkalis, and which destroys the hexagonal and cubic hydrates that confer cementitious properties to the binder. In this process, the carbonated alkalis (Na_2CO_3) formed by the combination of NaOH and CO_2 react with the hydrated calcium aluminates (CAH_{10}, C_2AH_8, C_3AH_6) to form soluble alkali aluminates.

The scientific community has been seeking alternatives to mitigate the durability problems associated with CAC cements (conversion, carbonation and alkaline hydrolysis). Authors such as Pacewska et al. [16] and Hidalgo et al. [13] introduced into the cement system appropriate additions of spent catalyst FCC [16], and silica fume or fly ash [13] to stabilise CAC hydrates and to avoid, or to at least reduce, their conversion and negative effects on CAC composites. An alternative reaction for metastable hydrates was observed in both the above studies, with silicate ions reacting with calcium aluminate hydrates (CAH_{10}–C_2AH_8) to form Strätlingite (C_2ASH_8), a stable hydrate formed within the normal temperature range. In [10], metakaolin and CAC blends were alkali-activated with NaOH and sodium silicate solutions. None of the compounds normally observed in water-hydrated CAC (CAH_{10}, C_2AH_8, C_3AH_6, AH_3) was detected under the study conditions (curing at 85ºC for 2 or 20 h), and the Al and Ca from CAC were taken up in the aluminosilicate gel formed in the activation process. Through the hydration of CAC with NaOH solutions, Pastor et al. [17] also found that alkali activation accelerated the conversion process to yield the cubic aluminate hydrate from very early ages (2 days in samples activated with 8 M and 12 M NaOH), instead of the hexagonal aluminates (CAH_{10} and C_2AH_8) that appeared during standard water hydration. These results have been corroborated in [18] by CAC hydration with highly alkaline NaOH (8M) and sodium silicate solutions, where

high pH values resulted in the formation of cubic hydrates from the outset, and no C_2ASH_8 was formed since silicon was taken up to form katoite-type phases ($C_3AS_nH_m$).

The work reported herein aims to understand the influence of calcium aluminate cement (CAC) additions and curing temperature on the mechanical strength and microstructure evolution of alkali-activated red clay brick waste (RCBW) cements. RCBW was partially replaced with CAC (0 to 50 wt.%), and blends were activated with NaOH/sodium silicate solutions and cured at room temperature and at 65ºC. .

2. Experimental Procedure

2.1. Materials

The studied samples were prepared with red clay brick waste (RCBW) and calcium aluminate cement (CAC), the latter produced by the company Cementos Molins S.A. (Barcelona, Spain). Red clay bricks were crushed in a jaw crusher (BB200, Retsch) to obtain a granular material with a particle size of less than 4 mm. This was then dry-milled in alumina media for 40 minutes, and powder with a mean particle size close to 21 µm and 90 vol.% less than 56.2 µm was obtained (determined by laser diffraction in a Mastersizer 2000, Malvern Instruments). The CAC particle size was similar, with a mean diameter of 27.7 µm and 90 vol.% under 64.3 µm. According to the SEM images in Fig. 1, both RCBW and CAC particles were irregularly shaped.

The chemical composition of RCBW and CAC, determined by X-ray fluorescence (XRF, Philips Magix Pro), is provided in Table I. While CAC is composed mainly of Al_2O_3 and CaO, RCBW contains high levels of SiO_2 and Al_2O_3, which are essential for the alkali-activation process. The amorphous content of RCBW, determined following UNE EN 196-2, was around 35%.

Table 1. Chemical composition of raw materials, wt.%

Oxide	RCBW	CAC
SiO_2	49.9	4.9
Al_2O_3	16.6	37.1
Fe_2O_3	6.5	15.6
CaO	9.7	35.4
MgO	5.5	1.3
Na_2O	0.5	0.6
TiO_2	0.8	2.4
SO_3	3.3	0.7
K_2O	4.4	0.7
Other	0.4	0.3
LOI	2.4	1.0

2.2. Matrix Preparation

Different percentages of calcium aluminate cement (0 to 50 wt.%) were used to substitute ceramic waste. The alkali-activating solutions were prepared by mixing sodium hydroxide pellets (98% purity, Panreac), water and sodium silicate (Merck, SiO_2=28%, Na_2O=8%, H_2O=64%). The activating solution dosage (SiO_2/Na_2O molar ratio of 1.60) was adopted from previous studies [9] and was kept constant for all the pastes and mortars mixed. A water to binder ratio (w/b) of 0.40 was used in the present research, which was lower than that previously reported in [9] due to the better workability of the RCBW-CAC blended mortars. A water-hydrated CAC paste (w/b 0.35) was prepared for comparison.

Pastes and mortars were produced according to the process previously described in [9,19]. They were cured in a thermostatically-controlled bath at 65ºC at a relative humidity (RH) of 96% for 3 and 7 days; and in a room temperature chamber (20ºC, RH 96%) for 3, 7, 14 and 28 days. A sand to binder (sum of CAC plus RCBW) ratio of 3:1 was used for all the prepared mortars. The process variables used in this study are summarised in Table 2.

Table 2. Dosages and curing conditions of pastes and mortars

RCBW wt.%	CAC wt.%	w/b	SiO_2/Na_2O molar ratio	Sand/binder	Curing conditions
100	0	0.40	1.60	3:1	3 and 7 days 65ºC
90	10				
80	20				
70	30				
60	40				
50	50				
100	0	0.40	1.60	3:1	3, 7, 14 and 28 days 20ºC
90	10				
80	20				
70	30				
60	40				
50	50				
0	100	0.35	-	-	

2.3. Characterisation

The compressive strengths of the alkali-activated mortars were determined following UNE EN 196-1 using 160 x 40 x 40 mm samples. Pastes were used to assess the microstructure evolution of the developed samples. Thermogravimetry tests (TG, 850 Mettler-Toledo) were run in sealed pin-holed aluminium crucibles at a heating rate of 10ºC min^{-1}, from 35ºC to 600ºC, in an N_2 atmosphere. X-ray diffraction tests (XRD, Brucker AXS D8 Advance) were run from 5º to 55º 2θ degrees, with Cu Kα radiation at 40 kv and 20 mA. The Fourier-transformed infrared spectroscopy (FTIR, Bruker Tensor 27 Platinum ATR spectrometer) data were collected in the transmittance mode, from 4,000 to 400 cm^{-1}. Water/binder suspensions were monitored by

electrical conductivity and pH measurements (microCM2201 conductimeter and micropH2001 pH-meter by Crison). These analyses were performed by dissolving 1g of paste with 10 ml of distilled water for 10 min. Data were taken from 1 day up to the maximum curing age established in the present study (28 days at 20ºC and 7 days at 65ºC). The microstructure of the alkali-activated RCBW-CAC paste samples was examined using SEM–EDX (JEOL JSM-6300).

3. Results and Discussion

3.1. Mechanical Strength

The evolution of the compressive strength of the alkali-activated RCBW-CAC blended mortars, cured at room temperature and at 65ºC for different periods of time is depicted in Fig. 2. The mortars with 50 wt.% CAC did not develop since rapid setting occurred in the preparation process. The alkali-activated RCBW mortar with no CAC addition required high temperature curing conditions to initiate the chemical reactions associated with the alkali-activation process. While only 10 MPa were achieved after 28 curing days at room temperature, this value increased up to 35 MPa after curing at 65ºC for 7 days. Conversely, although the mortars cured at 65ºC always exhibited higher compressive strength values than that cured at room temperature, the mechanical properties of that containing CAC were similar after 28 days at 20ºC or 7 days at 65ºC, no matter what the CAC addition.

The mechanical properties of all the prepared mortars increased with CAC addition. Although the kinetics of the room temperature process was quite slow for the samples containing 10 wt.% CAC (≈15 MPa, 7 curing days), more than 30 MPa were achieved after 28 curing days. Increasing CAC content to 20 wt.% significantly improved compressive strength, with 38 MPa and 55 MPa being achieved after 7 and 28 curing days, respectively. The values obtained for the greatest CAC additions (40 wt.%) came close to 80 MPa (28 days at 20ºC), which fall within

the range previously reported by Fernandez-Jimenez et al. [18] and Pastor et al. [17] in alkali-hydrated CAC pastes activated with 8M NaOH solutions and cured at room temperature for 28 days. Increased strength with curing time was also observed in both studies [17,18], which is in good agreement with the obtained results.

3.2. Evolution of pH and electrical conductivity

The reaction processes of the developed samples were monitored by electrical conductivity and pH measurements. Pastes were dissolved in distilled water for 10 minutes, and data were collected every 4 h on curing day 1 and at the different curing ages, established to assess compressive strength evolution (3 and 7 days at 65ºC; 3, 7, 14 and 28 days at room temperature). Fresh RCBW-CAC samples showed an initial electrical conductivity of 18.1-20.3 mS/cm. These values significantly decreased after 3 curing days to yield values within the range of 14.3-17.8 mS/cm at 20ºC, and 9.8-12.6 mS/cm at 65ºC. In general, the values of the activated pastes cured at room temperature were slightly higher than those cured at 65ºC for all the testing ages, which is attributed to the slower reactivity of the pastes cured at room temperature. From 3 to 28 days curing days at 20ºC, electrical conductivity decreased to the 11.1-14.2 mS/cm range, suggesting a continuous reaction in these systems. Generally, the electrical conductivity values found for the highest CAC content samples (30 wt.% and 50 wt.%) were slightly higher than those found for that containing 0 wt.% and 10 wt.% CAC. However, the differences between the RCBW paste (0 wt.% of CAC) and that containing 50 wt.% CAC were not significant, which suggests that the alkali solution reacted with both materials (ceramic waste and cement). According to Tashima et al. [3], the lower conductivity observed with curing time is attributed to the chemical combination of Na^+, OH^- groups and silicate anions while the alkali-activated matrix formed. Furthermore, CAC probably reacted with a smaller quantity of ions in the activating solution to leave more ions in the pore solution. Water-hydrated CAC cement exhibited the lowest electrical conductivity values (2.57 mS/cm in fresh state, which lowered to 1.57 mS/cm after 24 h of curing at room temperature), and slightly reduced to 1.42 mS/cm after 28 curing days.

Alkali-activated CAC blended pastes presented pH values that ranged from 12.3 to 12.8. The data collected immediately after the mixing process (12.8 for 50 wt.% CAC and 12.6 for 0 wt.% CAC) gave slightly lower values with curing time, which ranged from 12.6 (50 wt.% CAC) to 12.3 (0 wt.% CAC) after 28 curing days at 20ºC or 7 days at 65ºC. Similarly to the electrical conductivity behaviour, the water-hydrated CAC paste obtained the lowest pH values, which went 11.8 right immediately being mixed, to 11.5 after 28 curing days at 20ºC. As previously observed in the studies by Pastor et al. and Shi et al. [2,17], high pH values slow down the dissolution rate of Ca and accelerate that of Al and Si, which influences the developed microstructure. Yet according to Garcia Lodeiro et al. [20], the presence of calcium also modifies the structure of N-A-S-H gels by replacing part of the sodium with calcium to form (N,C)-A-S-H gels. The stability of these structures in the presence of calcium depends heavily on pH; thus if sufficient calcium is provided, pH values of over 12 promote the formation of C-A-S-H rather than N-A-S-H gel.

3.3. Infrared spectroscopy (FTIR)

The FTIR curves of the alkali-activated RCBW-CAC blends, cured at 20ºC for 28 days and at 65ºC for 7 days, are plotted in Fig. 3a and 3b, respectively. The spectrum of the water-hydrated CAC paste, cured at room temperature, is also presented for comparison purposes. The presence of quartz, also identified by XRD (Section 3.4), was corroborated in all the RCBW-containing samples, and was associated with the signals appearing at 460 cm^{-1}, 668 cm^{-1}, 697 cm^{-1}, 796-778 (double band) cm^{-1}, 1084 $cm^{-1}$and 1150 cm^{-1} [21,22], with decreasing intensity with higher CAC additions.

The FTIR spectra may be difficult to identify since bands attributed to different compounds tend to overlap. As reported in [16,17,21,23], the bands attributed to AH_3 appear at 3475, 3530 and

3630 cm^{-1} (O-H stretching vibration) and in the 1027 and 990-970 cm^{-1} region (O-H bending vibration), and overlap that typical of CAC hydrates and the newly formed aluminosilicate gel, respectively. As explained in [17,21], the high frequency bands of CAH_{10} (3500 cm^{-1}), C_2AH_8 and C_3AH_6 (narrow band at 3665 cm^{-1}) hydrates also overlap since they present very similar spectra [21,24]. The signals appearing at 3465, 3525 and 3620 cm^{-1} in the water-hydrated CAC paste, whose intensity increased with curing time, are attributed to both gibbsite and CAC hydrates. The bands assigned typically to CAC hydrates (CAH_{10}, C_2AH_8 and C_3AH_6), which appear at 524 cm^{-1} and in the 3465 - 3670 cm^{-1} region [24], were not clearly distinguished by the FTIR analyses in the alkali-activated RCBW-CAC samples. Only a slight tendency within the 3,200 to 3,600 cm^{-1} range was observed with increasing CAC additions, which implies that no significant amounts of these hydrates were formed. The results are in good agreement with those reported by Shi et al. [2], who stated that when less than 30% CAC is used in alkali-activated calcium aluminate-blended cements, CAC does not undergo normal hydration, and no cubic, hexagonal hydrates or $Al(OH)_3$ are observed since Al and Ca of CAC are taken up in the (C,N)-A-S-H gel formed. Pastor et al. [17] and Fernandez-Jimenez et al.[18], who activated CAC, also observed that highly alkaline solutions expedite the conversion from hexagonal into cubic hydrates, which results in katoite formation (C_3AH_6) from the outset.

Several papers [13,16,18] have also addressed CAC hydration with water in the presence of reactive silica-rich compounds (slag, silica fume, fly ash, etc.). Most of these papers reported that metaestable calcium aluminates (CAH_{10} and C_2AH_8) react with added silica to form strätlingite (C_2ASH_8), a stable crystalline hydrate that inhibits or retards the conversion from hexagonal into cubic hydrates [18]. However, FTIR or XRD analyses in the present study detected no strätlingite, which is attributed to the fact that no significant amounts of typical CAC hydrates formed in the activated samples. These results are also in good agreement with those previously reported by Fernandez-Jimenez et al. [18], who did not observe C_2ASH_8 formation when activating CAC in highly alkaline solutions and in the presence of soluble silica. According to [18], these conditions favour the reaction between the silica and aluminum and calcium in CAC to produce a sodium and calcium aluminosilicate hydrate (C,N–A–S–H) gel, which may

crystallise into zeolitic phases. These authors also found that silicon is taken up to form katoite-type phases ($C_3AS_nH_m$). However, the main bands attributed to $C_3AS_3–xH_{2x}$ solid solution hydrates are difficult to identify by FTIR tests since, as reported by Hidalgo et al. [13], they occur at 3,660, 900 and 550 cm $^{-1}$, and overlap that of typical CAC hydration products and the newly-formed gel.

All the alkali-activated samples showed a broad band centred at ≈1,000 cm^{-1}, which has been attributed to the vibrations of the Si–O–T (T = Al, Si) bonds in the newly formed aluminosilicate gel [18]. A slight deviation towards lower wave numbers with increasing CAC contents was observed, which indicates more Al contents [21,25]. The signal that appears in the 460 cm^{-1} region also slightly shifted towards lower wave numbers with more CAC additions. Although this signal is attributed mainly to quartz, bands due to the deformation vibrations of C-A-S-H and N-A-S-H gels (δ Si-O-Si / δ Si-O-Al) also appear in this region [26]. As explained by García-Lodeiro et al. [26,27], the type and characteristics of the formed gel are conditioned clearly by the working pH and the calcium concentration in the system. Thus even in the presence of Ca, N-A-S-H persists with pH values below 12, and by accepting Ca by an ion exchange mechanism to confer (N,C)-A-S-H until all the Na has been replaced with Ca (if sufficient Ca is available). However, pH values of over 12 favour the formation of a C-A-S-H rather than a N-A-S-H gel, given that sufficient calcium is provided. According to Juenger et al. [1], while the C–(A)–S–H gel is amorphous to partially crystalline, the geopolymer-type gel N-A-S-H is a highly cross-linked aluminosilicate gel that strongly resembles zeolite frameworks nanostructurally and is generally lacking in the long-range crystalline order. Garcia-Lodeiro et al. [20] also agreed that the alkaline activation of low calcium materials, such as metakaolin, leads to N-A-S-H gel precipitation, which provides zeolites such as hydroxysodalite, zeolite P, Na-chabazite, zeolite Y or faujasite as secondary reaction products. These observations, together with the fact that no significant amounts of zeolitic-type products were clearly distinguished by the XRD or FTIR analyses in RCBW-CAC blended systems (characteristic bands at 660 and 720 cm^{-1} [28]), led to the conclusion that (N,C)-A-S-H rather than a N-A-S-H gel is being formed, with increasing C-A-S-H contents if there are more CAC additions.

According to [16,22,24], the bands appearing from 1,415 cm^{-1} to 1,600 cm^{-1} are associated with the stretching vibrations of CO_3^{-2} in carbonates. The intensity of these bands was higher in the pastes cured at room temperature than that cured at 65ºC. While calcite-type bands appear at lower wave numbers (1420 cm^{-1}), that of carbonate impurity species shift to higher values (Natrite, Na_2CO_3, 1,455 cm^{-1}; vaterite, 1,484 cm^{-1} [17]), which denotes higher calcite-type compounds with increasing CAC additions. The absorption bands at 712 and 875 cm^{-1}, when connected with the distinct bands at about 1,420 cm^{-1}, are also related to carbonate salts [16]. Pastor et al. [17] observed an increasing intensity of the bands attributed to carbonates with curing time in alkali-activated CAC, together with increasing AH_3 contents and a decline in the C_3AH_6 hydrate. It was not possible to corroborate this evolution by FTIR analyses in the present study since the signals attributed to both AH_3 and CAC hydrates overlapped in the 3,200 to 3,600 cm^{-1} region, and they did not vary significantly with curing time. The signals attributed to hydrated calcium monocarboaluminate $3CaO{\cdot}Al_2O_3{\cdot}CaCO_3{\cdot}11H_2O$, a metastable intermediate specie in the carbonation process identified by XRD analyses, also appeared in the 3,760 cm^{-1} region [13], which is difficult to identify by FTIR. Although the formation of further calcite contents with CAC addition may be linked to the alkaline hydrolysis process, no significant amounts of typical CAC hydrates were identified by FTIR or XRD analyses, especially in the samples containing up to 10 wt.% CAC. During alkaline hydrolysis, the hydrated calcium aluminates react with carbonated alkalis (Na_2CO_3) to give $CaCO_3$ and soluble alkaline aluminate $Na_2O{\cdot}Al_2O_3$ [14]. This aluminate reacts with water and renders new alkaline hydroxides that maintain the CAC hydrates destruction process.

3.4. X-ray diffraction (XRD)

The results of XRD analyses obtained for the pastes cured at 20ºC for 28 days and at 65ºC for 7 days are presented in Fig. 4a and 4b, respectively. The RCBW diffractogram is plotted for comparison purposes. The data show that quartz (SiO_2, PDFcard331161) is the major crystalline phase to appear in the raw material, with the calcium silicate rankinite ($2SiO_2.3CaO$, PDFcard220539), and the feldspars albite ($NaAlSi_3O_8$, PDFcard090466) and microcline

($KAlSi_3O_8$, PDFcard090466) present as minor constituents. Typical CAC hydrates (CAH_{10}, C_2AH_8 and C_3AH_6), together with the crystalline phase gibbsite (AH_3), were clearly identified in the water-hydrated CAC paste. This sample also contained unreacted clinker phases of cement, type monocalcium aluminate ($CaO{\cdot}Al_2O_3$, PDFcard231036) and small amounts of carboaluminate phase $Ca_4Al_2O_6CO_3{\cdot}11H_2O$ (PDFcard410219).

The signals attributed to quartz appeared in all the samples containing RCBW, with decreasing intensity if CAC contents increased, due to the dilution effect in the RCBW-CAC systems. A deviation from the baseline within the 20 to 35 2θ degrees range was observed in all the alkali-activated samples, which augmented with CAC addition and denotes the further development of amorphous phases. Only the crystalline phases that were attributed to the raw material were clearly identified in the pastes containing up to 10 wt.% CAC and cured at 20ºC. Monocalcium aluminate was observed with increasing CAC contents (30 and 50 wt.%, cured at 20ºC), together with minor amounts of carboaluminate phase aluminohydrocalcite ($CaAl_2(CO_3)_2(OH)_4{\cdot}3H_2O$, PDFcard220138), whose signals intensified with CAC addition.

The XRD spectra of the alkali-activated pastes blended with 0 wt.% and 10 wt.% CAC cured at 65ºC were similar to that cured at room temperature. Although zeolitic phase Herschelite ($NaAlSi_2O_6{\cdot}3H_2O$, PDFcard191178) was identified in the paste mixed with 10 wt.% CAC, it disappeared with increasing CAC contents (30 and 50 wt.%), and minor amounts of cubic phase katoite (C_3AH_6, PDFcard240217) appeared with a higher intensity with CAC addition. Minor amounts of AH_3 polymorph bayerite (PDFcard200011), together with the formation of a new hydrated calcium silicoaluminate crystalline phase ($Ca_6(AlSiO_4)_{12}{\cdot}30H_2O$, PDFcard110589), were formed in the paste containing 50 wt.% CAC.

The X-ray results are in good agreement with those obtained in the FTIR and TG analyses since no crystalline gibbsite or hexagonal hydrates were clearly identified in the alkali-activated RCBW-CAC blended samples, and the phase bayerite was only observed in the paste containing 50 wt.% CAC and cured at 65ºC for 7 days. Cubic phase katoite (C_3AH_6) was

detected only in the pastes blended with high CAC contents (30 wt.% and 50 wt.%) cured at 65ºC. The results are in accordance with the previous review by Shi et al. [2], which pointed out that alkali-activated CAC blended cements do not undergo normal hydration and, instead of cubic or hexagonal typical CAC hydrates being formed, Al and Ca were taken up in the N-A-S-H gel to confer (N,C)-A-S-H or C-A-S-H gels depending on the blend proportions and reaction conditions. Pastor et al. [17] also detected an alternative reaction form in the NaOH-hydrated CAC samples, which led to the formation of cubic hydrate C_3AH_6 and AH_3 instead of hexagonal aluminates (CAH_{10} and C_2AH_8), which usually appear during standard water hydration. Neither were hexagonal hydrates found in the study by Fernandez Jimenez et al. [18], where CAC was hydrated in NaOH and sodium silicate solutions. While cubic phase C_3AH_6 was identified in the alkali-activated pastes with no silica addition, presence of this compound was found to interact with C_3AH_6 to form $Ca_{2.93}Al_{1.97}(Si_{0.64}O_{2.56})(OH)_{9.44}$ and the calcium aluminum silicate hydrate, known as Linde A (Ca_6 $(AlSiO_4)_{12}\cdot 30H_2O$, ICDD-11-0589) [18], which was also identified by the XRD tests in the paste developed in the present research work blended with 50 wt.% CAC and cured at 65ºC for 7 days.

3.5. Thermal analysis (DTA/TG)

The differential thermogravimetric curves (DTG) of the alkali-activated RCBW-CAC blends, cured at 20ºC for 28 days and at 65ºC for 7 days are plotted in Fig. 5a and 5b, respectively. Total weight loss generally increased with CAC addition and curing time, and ranged from 7.4 wt.% to 9.0 wt.% in the pastes cured for 3 days at 20ºC (0 wt.% and 50 wt.% CAC, respectively), up to 8.9 wt.% (0 wt.% CAC) to 11.7 wt.% (50 wt.% CAC) in those cured for 28 days. Values were slightly higher in the pastes cured at 65ºC for 7 days (10.2 wt.% in 0 wt.% CAC to 12.5 wt.% in 50 wt.% CAC), which is attributed to faster reaction progress. These results are in good agreement with compressive strength evolution.

A water-hydrated CAC paste, cured at room temperature, was tested for comparison purposes. While the first peak appearing on the DTG curve (130 ºC), which is associated with the dehydration of the C-A-H and alumina gel [23,26], increased with curing time, the second one (150ºC to 180ºC), which corresponds to the dehydration of CAH_{10} and C_2AH_8 [16,23], was maximum after 14 curing days, but decreased afterwards, indicating that the conversion process occurred. The bands that appeared within the 180-220ºC range, whose intensity increased with curing time, are associated with the dehydration of carboaluminate phases and further C_2AH_8 dehydration. The intensity of the signal due to the dehydration of gibbsite AH_3 (309 ºC) [16,23] also increased with curing time, and that associated with C_3AH_6 cubic compounds (≈340 ºC) [16] appeared after 7 curing days and increased to 28 days.

The thermogravimetric curves of the alkali-activated pastes with no CAC or with 10 wt.% addition exhibited a single broad band centred at 140-160ºC which, according to Tashima et al. [3], is attributed to the dehydration of the newly-formed gel, originated by loss of water molecules and/or OH^- groups from the products formed in the alkali-activation process. Zeolitic phase Herschelite, which was previously identified by the XRD tests in the pastes blended with 10 wt.% CAC and cured at 65ºC for 7 days, was not clearly distinguished by the TG analyses since the dehydration of zeolitic type products also appeared within this temperature range (60 - 160ºC) [29]. The alkali-activated gel band progressively broadened with increasing CAC contents, which is attributed to a different composition of the newly-formed gel. The pastes containing 50 wt.% CAC exhibited a double peak in this region, which denotes the overlapping dehydration processes of different calcium aluminum silicate hydrates. No signals attributed to carbonates were identified by the TG analyses since, according to Hidalgo et al. [13], bands appear within the 625ºC to 875ºC temperature range.

In good agreement with the XRD results, the signal originated by the C_3AH_6 phase (≈340 ºC) [16] was clearly identified only in the activated pastes containing 30 wt.% and 50 wt.% CAC cured at 65ºC, which showed increasing intensity with more CAC contents. Although a slight

deviation within this range appeared in the DTG curve for the 50 wt.% CAC blended paste cured at 20ºC, the XRD analyses did not clearly distinguish the cubic phase in this sample.

3.6. Scanning electron microscopy (SEM)

The SEM micrographs of the alkali-activated RCBW-CAC blends containing 10 wt.% and 50 wt.% CAC, cured at 20ºC for 28 days and at 65ºC for 7 days, are shown in Fig. 6. A denser microstructure was observed with increasing CAC contents, which is in good agreement with the compressive strength results. Although no cubic hydrates were clearly identified by the FTIR, XRD or TG analyses in the samples containing 10 wt.% CAC, minor amounts of this phase were observed by SEM. Despite a most particular microstructure having developed in the blended pastes containing 50 wt.% CAC and cured at 65ºC, no mortars with this amount of CAC were obtained since rapid setting occurred in the preparation process.

4. Conclusions

An alternative cementitious system has been developed at both room temperature and 65ºC by the alkali activation of red clay brick waste in the presence of calcium aluminate cement. The conclusions drawn according to the results of this paper are listed below.

- Addition of calcium aluminate cement accelerates the alkali-activation process of red clay brick waste, which is particularly important for the mortars cured at room temperature. While up to 50 MPa were obtained under compression after 3 curing days at 20ºC with 40 wt.% CAC, similar compressive strength values were obtained in the mortars that contained 20 wt.% CAC after 28 curing days.

- Compressive strength values increased with CAC addition, curing temperature and curing time. Although the mortars that contained 50 wt% CAC rapidly set and could not be prepared, up to 92 MPa were obtained in the blend with 40 wt.% CAC that was cured at 65ºC for 7 days .

- The main reaction product was a cementitious gel containing Ca and Al from CAC. CAC did not undergo normal hydration and, while the cubic phase C_3AH_6 was identified only in the pastes containing the largest CAC amounts (30 wt.% and 50 wt.%) cured at 65ºC, bayerite was distinguished only in the system with 50 wt.% CAC (65ºC). Thus the typical durability problems associated with CAC hydrates (conversion, carbonation, alkaline hydrolysis) are not expected in the alkali-activated RCBW/CAC systems blended with up to 20 wt.% CAC, no matter what the curing temperature may be.

Acknowledgements

The authors are grateful to the Spanish Ministry of Science and Innovation for supporting this study through Project GEOCEDEM BIA 2011-26947, and to FEDER funding.

References

[1] Juenger MCG, Winnefeld F, Provis JL, Ideker JH. Advances in alternative cementitious binders. Cem Concr Res 2011;41:1232–1243.

[2] Shi C, Fernández-Jiménez A, Palomo A. New cements for the 21st century: The pursuit of an alternative to Portland cement. Cem Concr Res 2011;41:750–763.

[3] Tashima MM, Akasaki JL, Castaldelli VN, Soriano L, Monzó J, Payá J, Borrachero MV. New geopolymeric binder based on fluid catalytic cracking catalyst residue (FCC). Mater Lett 2012;80:50–52.

[4] Redden R, Neithalath N. Microstructure, strength, and moisture stability of alkali activated glass powder-based binders. Cem Concr Compos 2014;45:46-56.

[5] Gluth GJG, Lehmann C, Rübner K, Kühne HC. Reaction products and strength development of wastepaper sludge ash and the influence of alkalis. Cem Concr Compos 2014;45:82-88.

[6] Puertas F, Barba A, Gazulla MF, Gómez MP, Palacios M, Martínez-Ramírez S. Ceramic wastes as raw materials in portland cement clinker fabrication: characterization and alkaline activation. Mater Construcc 2006;56(281):73-84.

[7] Payá J, Borrachero MV, Monzó J, Soriano L, Tashima MM. A new geopolymeric binder from hydrated-carbonated cement. Mater Lett 2012;74:223-225.

[8] Reig L, Soriano L, Borrachero MV, Monzó J, Payá J. Influence of the activator concentration and calcium hydroxide addition on the properties of alkali-activated porcelain stoneware. Constr Build Mater 2014;63:214–222.

[9] Reig L, Tashima MM, Borrachero MV, Monzó J, Cheeseman CR, Payá J. Properties and microstructure of alkali-activated red clay brick waste. Constr Build Mater 2013;43:98–106.

[10] Fernández-Jiménez A, Palomo A, Vazquez T, Vallepu R, Terai T, Ikeda K. Alkaline activation of blends of metakaolin and calcium aluminate. J Am Ceram Soc 2008;91(4):1231–1236.

[11] Arbi K, Palomo A, Fernández-Jiménez A. Alkali-activated blends of calcium aluminate cement and slag/diatomite. Ceram Int 2013;39:9237–9245.

[12] Pacewska B, Nowacka M, Antonovic V, Aleknevicius M. Investigation of early hydration of high aluminate cement-based binder at different ambient temperatures. J Therm Anal Calorim 2012;109:717–726.

[13] Hidalgo A, García JL, Alonso MC, Fernández L, Andrade C. Microstructure development in mixes of calcium aluminate cement with silica fume or fly ash. J Therm Anal Calorim 2009;96(2):335–345.

[14] Giner-Juan FJ. Carbonatación vs. Aluminosis. In: Proceedings of the 'V Convención Técnica y Tecnológica de la Arquitectura Técnica', ContART 2009, Albacete-Spain, March, 2009. p. 25-27.

[15] Rivas-Mercury JM, de Aza AH, Turrillas X, Pena P. Hidratación de los cementos de aluminatos de calcio (Parte I). Bol Soc Esp Cerám Vidrio 2003;42(5):269-276.

[16] Pacewska B, Nowacka M, Wilinska I, Kubissa W, Antonovich V. Studies on the influence of spent FCC catalyst on hydration of calcium aluminate cements at ambient temperature. J Therm Anal Calorim 2011;105:129–140.

[17] Pastor C, Fernández-Jiménez A, Vázquez T, Palomo A. Calcium aluminate cement hydration in a high alkalinity environment. Mater Construcc 2009;59(293):21-34.

[18] Fernández-Jiménez A, Vázquez T, Palomo A. Effect of sodium silicate on calcium aluminate cement hydration in highly alkaline media: a microestructural characterization. J Am Ceram Soc 2011;94(4):1297–1303.

[19] Reig L, Tashima MM, Soriano L, Borrachero MV, Monzó J, Payá J. Alkaline activation of ceramic waste materials. Waste Biomass Valor 2013;4(4):729–736.

[20] García-Lodeiro I, Maltseva O, Palomo A, Fernández-Jiménez A. Hybrid alkaline cements. Part I: Fundamentals. Rom J Mater 2012;42(4):330-335.

[21] Fernández-Carrasco L, Vázquez E. Reactions of fly ash with calcium aluminate cement and calcium sulphate. Fuel 2009;88:1533–1538.

[22] Fernández-Carrasco L, Torréns-Martín D, Martínez-Ramírez S. Carbonation of ternary building cementing materials. Cem Concr Compos 2012;34:1180–1186.

[23] Pacewska B, Nowacka M, Antonovic V, Aleknevicius M. Investigation of early hydration of high aluminate cement-based binder at different ambient temperatures. J Therm Anal Calorim 2012;109:717–726.

[24] Fernández-Carrasco L, Vázquez T. Aplicación de la espectroscopia infrarroja al estudio de cemento aluminoso. Mater Construcc 1996;46(241):53-65.

[25] Hajimohammadi A, Provis JL, van Deventer JSJ. The effect of silica availability on the mechanism of geopolymerisation. Cem Concr Res 2011;41:210–216.

[26] Garcia-Lodeiro I, Palomo A, Fernández-Jiménez A, Macphee D.E. Compatibility studies between N-A-S-H and C-A-S-H gels. Study in the ternary diagram Na_2O–CaO–Al_2O_3–SiO_2–H_2O. Cem Concr Res 2011;41:923–931.

[27] García-Lodeiro I, Fernández-Jiménez A, Palomo A. Variation in hybrid cements over time. Alkaline activation of fly ash–Portland cement blends. Cem Concr Res 2013;52:112–122.

[28] Granizo ML, Alonso S, Blanco-Varela MT, Palomo A. Alkaline activation of metakaolin: effect of calcium hydroxide in the products of reaction. J Am Ceram Soc 2002;85(1):225–31.

[29] Bernal SA, Gutierrez RM, Provis JL, Rose V. Effect of silicate modulus and metakaolin incorporation on the carbonation of alkali silicate-activated slags. Cem Concr Res 2010;40:898–907.

LIST OF FIGURES:

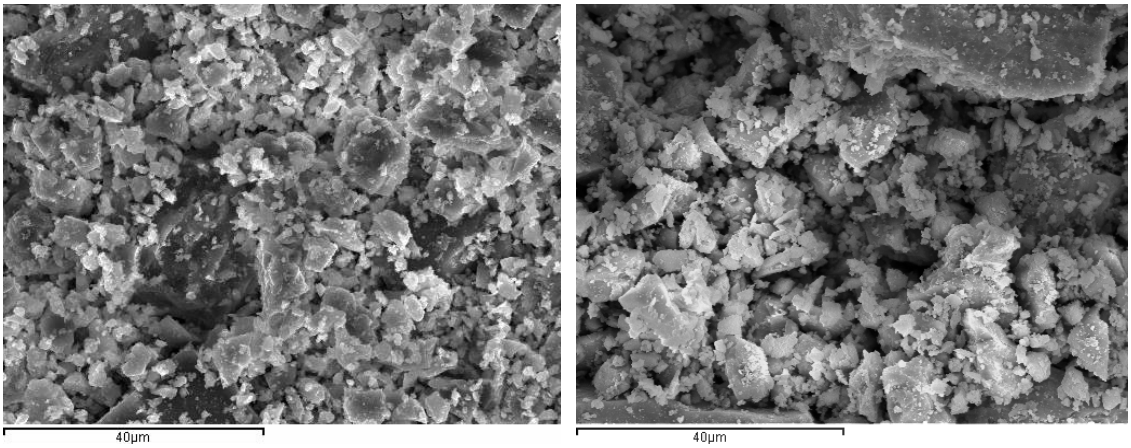

Fig. 1. SEM image of: a) Ground RCBW; b) CAC cement

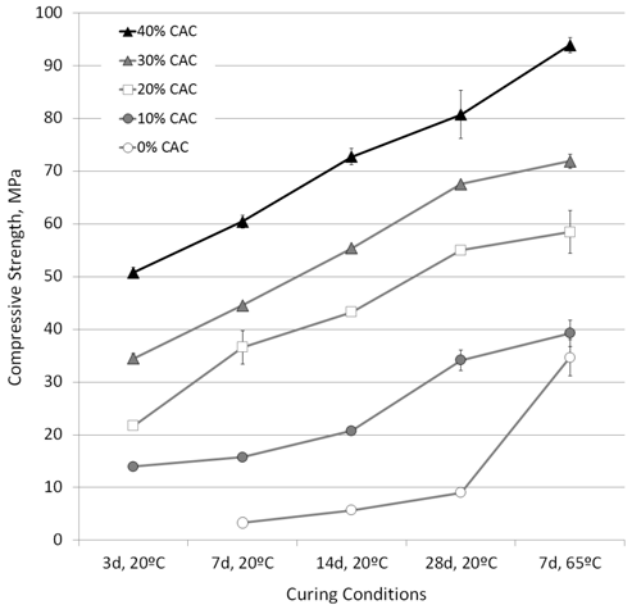

Fig. 2. Influence of CAC addition and curing conditions on the compressive strength of the alkali-activated RCBW-CAC mortars cured at 20ºC and 65ºC.

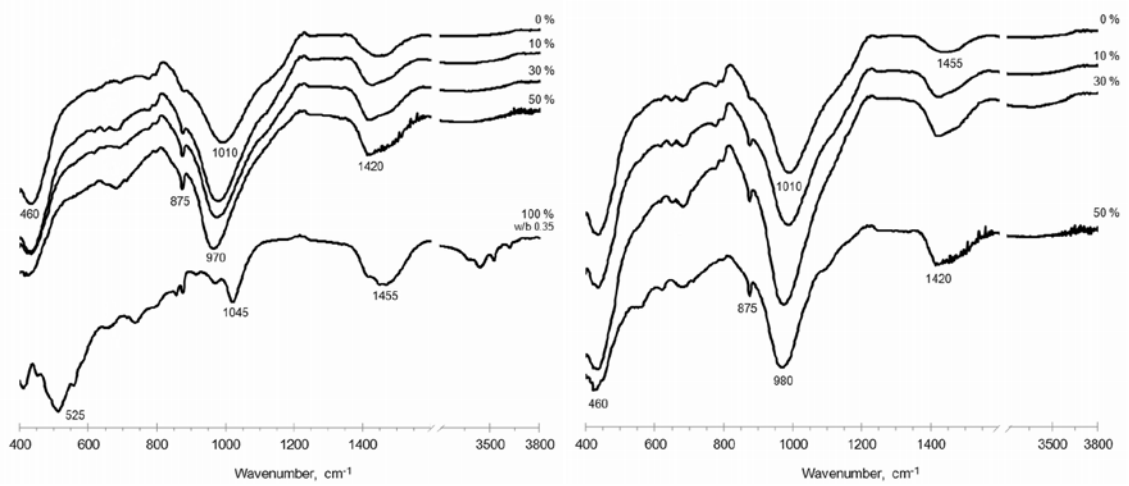

a b

Fig. 3. FTIR spectra for the alkali-activated RCBW-CAC blends and the hydrated CAC paste, cured at: a) 20ºC for 28 days; b) 65ºC for 7 days.

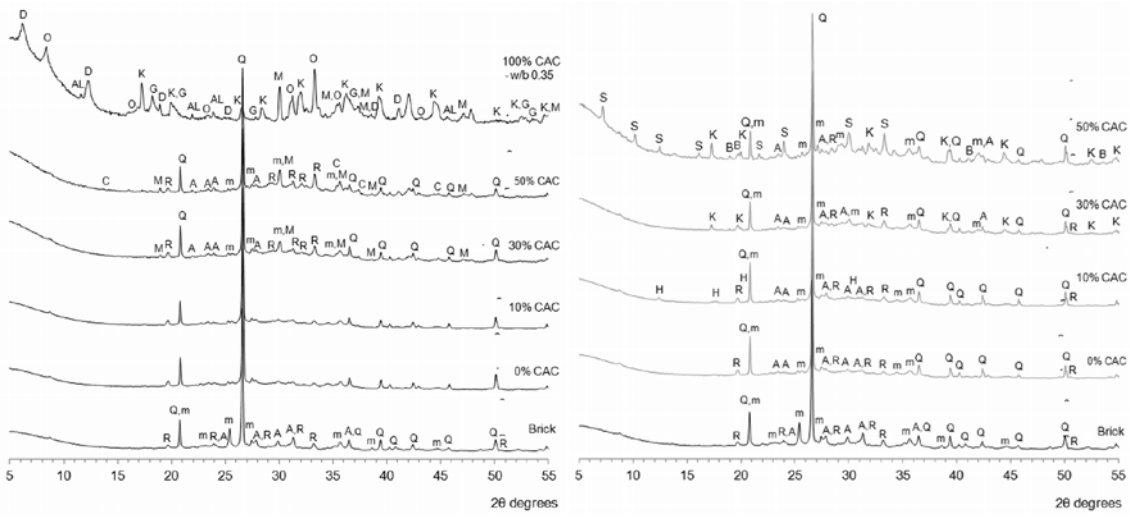

a b

Fig. 4. X-ray diffractograms for the alkali-activated RCBW-CAC blends and the water-hydrated CAC paste, cured at: a) 20ºC for 28 days; b) 65ºC for 7 days. Q=Quartz (SiO_2); A=Albite ($NaAlSi_3O_8$); m=microcline ($KAlSi_3O_8$); R=rankinite ($2SiO_2.3CaO$); M=monocalcium aluminate, CA ($CaO{\cdot}Al_2O_3$); D=CAH_{10} ($CaAl_2O_4{\cdot}10H_2O$); O=C_2AH_8 ($Ca_2Al_2O_5{\cdot}8H_2O$); K=katoite, C_3AH_6 ($Ca_3Al_2O_6{\cdot}6H_2O$); G=gibbsite ($Al(OH)_3$); B=bayerite ($Al(OH)_3$); S=Linde A, $Ca_6(AlSiO_4)_{12}{\cdot}30H_2O$; AL=carboaluminate ($Ca_4Al_2O_6CO_3{\cdot}11H_2O$); C=aluminohydrocalcite ($CaAl_2(CO_3)_2(OH)_4{\cdot}3H_2O$); H=Herschelite ($NaAlSi_2O_6{\cdot}3H_2O$).

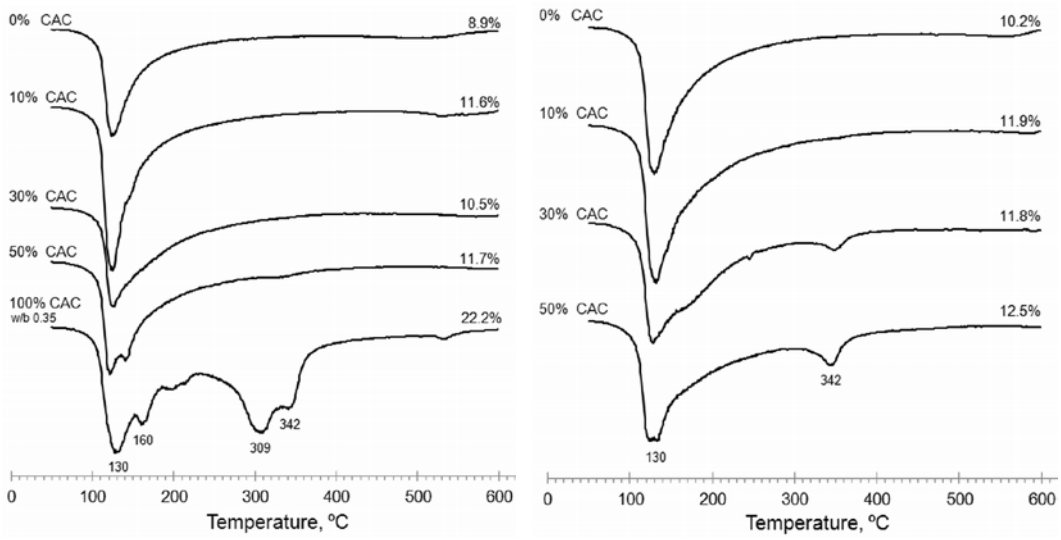

a b

Fig. 5. Differential thermogravimetric curves for the alkali-activated RCBW-CAC blends and a hydrated CAC paste: a) cured at 20ºC for 28 days; b) cured at 65ºC for 7 days. Total mass loss (as a %) within the 35-600ºC range is indicated for each curve.

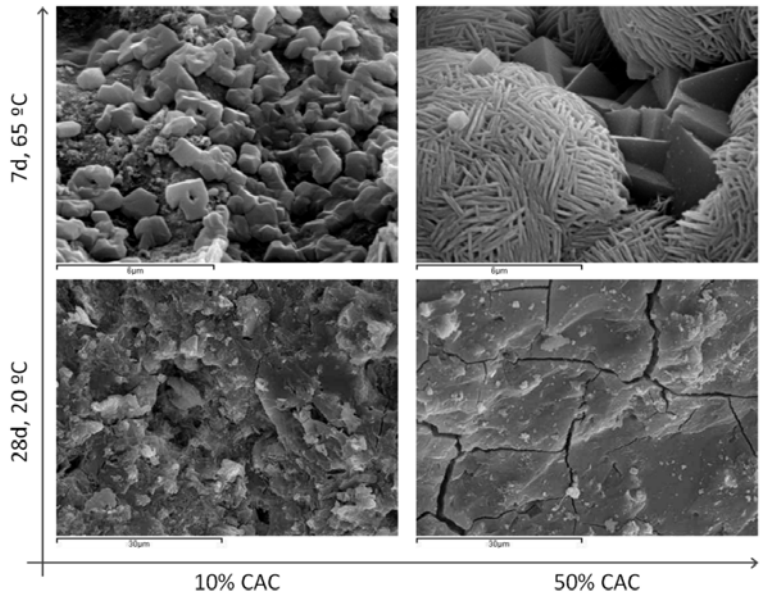

Fig. 6. Scanning electron microscope images of the alkali-activated RCBW-CAC blends cured at 20ºC for 28 days and 65ºC for 7 days.